This is an open access article published under a Creative Commons Non-Commercial No Derivative Works (CC-BY-NC-ND) Attribution License, which permits copying and redistribution of the article, and creation of adaptations, all for non-commercial purposes.

JACS
JOURNAL OF THE AMERICAN CHEMICAL SOCIETY
Article
pubs.acs.org/JACS

Infrared Transition Moment Orientational Analysis on the Structural Organization of the Distinct Molecular Subunits in Thin Layers of a High Mobility n-Type Copolymer

Arthur Markus Anton,*[,†] Robert Steyrleuthner,[§,‡] Wilhelm Kossack,[†] Dieter Neher,[‡] and Friedrich Kremer[†]

[†]Institut für Experimentelle Physik I, Universität Leipzig, Linnéstr. 5, 04103 Leipzig, Germany
[§]Institut für Experimentalphysik, Freie Universität Berlin, Arminallee 14, 14195 Berlin, Germany
[‡]Institut für Physik und Astronomie, Universität Potsdam, Karl-Liebknecht-Str. 24-25, 14476 Potsdam, Germany

Supporting Information

ABSTRACT: The IR-based method of infrared transition moment orientational analysis (IR-TMOA) is employed to unravel molecular order in thin layers of the semiconducting polymer poly[*N*,*N*′-bis(2-octyldodecyl)-1,4,5,8-naphthalene-diimide-2,6-diyl]-*alt*-5,5′-(2,2′-bithiophene) (P(NDI2OD-T2)). Structure-specific vibrational bands are analyzed in dependence on polarization *and* inclination of the sample with respect to the optical axis. By that the molecular order parameter tensor for the respective molecular moieties with regard to the sample coordinate system is deduced. Making use of the specificity of the IR spectral range, we are able to determine separately the orientation of atomistic planes defined through the naphthalenediimide (NDI) and bithiophene (T2) units relative to the substrate, and hence, relative to each other. A pronounced solvent effect is observed: While chlorobenzene causes the T2 planes to align preferentially parallel to the substrate at an angle of 29°, using a 1:1 chloronaphthalene:xylene mixture results in a reorientation of the T2 units from a *face on* into an *edge on* arrangement. In contrast the NDI unit remains unaffected. Additionally, for both solvents evidence is observed for the aggregation of chains in accord with recently published results obtained by UV−vis absorption spectroscopy.

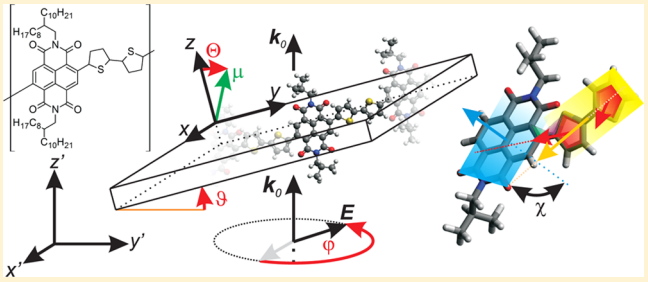

INTRODUCTION

Organic semiconducting polymers are in the focus of recent research and technological development, as organic light-emitting diodes and solar cells for instance, because of their specific and outstanding properties.[1] Conformational freedom of conjugated polymer chains gives rise to a large number of possible geometric arrangements while weak intermolecular interactions lead to poor structural order in the solid state.[2] Moreover, the morphology of those systems directly influences the electronic structure of the organic semiconductor, which is often accompanied by a significant variation of the charge carrier mobility. Thus, the transport of charges within the semiconductor represents one of the main limiting factors concerning the performance and efficiency of organic devices. A detailed characterization of the polymer film's microstructure on the molecular length scale, as well as its crystalline properties (coherent domain size and orientation) and the way that crystallites are embedded in the amorphous matrix is needed in order to be correlated with functional properties of photophysics or charge carrier transport.[3]

A class of materials that has drawn tremendous attention during the past years mainly motivated by their application as low band gap absorbers in organic solar cells are conjugated donor/acceptor-copolymers. In this study we are focusing on poly[*N*,*N*′-bis(2-octyldodecyl)-1,4,5,8-naphthalenediimide-2,6-diyl]-*alt*-5,5′-(2,2′-bithiophene) P(NDI2OD-T2) (ActivInk N2200, Polyera Corp., USA), originally introduced by Yan et al. in organic field effect transistors.[4] Because of its high and trap free electron mobility under ambient conditions,[4,5] it has been well established as electron conductor in n-type field effect transistors and as electron acceptor in polymer solar cell devices now reaching power conversion efficiencies of about 5.7%.[6−13]

Early work on thin P(NDI2OD-T2) films exhibit a distinct face-on orientation of the crystalline domains with respect to the substrate and significant signatures of $\pi-\pi$ stacking.[14] While this approach directly reveals the orientation of the crystallites, it is not possible to construct a unit cell in order to obtain the molecular structure or the orientation of the copolymer within the lattice. In addition optical, atomic force, and electron transmission microscopy visualize collective ordering up to a length scale of several micrometers for conventional spin coated films.[15−18] A combination of steady state UV−vis, photoluminescence, and nuclear magnetic resonance spectros-

Received: February 23, 2015
Published: April 20, 2015

 © 2015 American Chemical Society
DOI: 10.1021/jacs.5b01755
J. Am. Chem. Soc. 2015, 137, 6034−6043

Table 1. Overview of the Sample Names and According Preparation Parameters

sample name	solvent	substrate	annealed	thickness [nm]
CB	chlorobenzene	BaF_2	yes	2200 ± 100
CN:Xyl notA	chloronapthalene:xylene	BaF_2	no	1200 ± 100
CN:Xyl A	chloronapthalene:xylene	BaF_2	yes	1200 ± 100

copy shows that precursors of supramolecular assemblies (preaggregates) already present in polymer solution are mainly responsible for the structure formation in thin films.[19] Charge modulation spectroscopy and Kelvin-probe measurements give evidence for a low degree of energetic disorder in preaggregated P(NDI2OD-T2) films, which could be one reason for the good electron transport in this material.[20,21] In addition numerous studies investigated the influence of the crystallinity, crystallite orientation, preaggregation, aggregate content, and polymer regioregularity on the charge transport in P(NDI2OD-T2).[15,18,22−24] While charges can be efficiently transported along the polymer backbone or within the π stacks, it is believed that the long nonconjugated side chains represent a hopping barrier for charge transfer in this particular direction.[3] By controlling the P(NDI2OD-T2) thin film microstructure the electron mobility in bulk can be varied over 2 orders of magnitude illustrating the importance of coherent ordering for archiving good charge transport.[18] However, strongly disordered P(NDI2OD-T2) films still show reasonable electron transport which is attributed to the larger and more planar repeating units resulting in a structure more tolerant to disorder, as compared to poly(3-hexylthiophene) for example.[24] Larger aromatic units might also result in comparatively low reorganization energies upon charging the backbone calculated on DFT basis for P(NDI2OD-T2).[20,25] This demonstrates the need for experimental investigations on the molecular structure of the monomeric units as partial origin for the high mobility and its influence on functional material properties.

The occurrence of a specific dihedral angle between the two functional elements within a repeat unit seems to be characteristic for donor/acceptor copolymers as it has been demonstrated already in 2005 for DFT optimized structures of F8BT experimentally validated with Raman spectroscopy[26] and later on in FTIR experiments of conjugated homo- and copolymer films.[27−29] For P(NDI2OD-T2), quantum chemical calculations propose a planarization of the bithiophene (T2) rings with respect to the naphthalenediimide (NDI) unit when aggregating into the P(NDI2OD-T2) stack. This is believed to be the main reason for the concurrent red shift evident in optical absorption measurements.[19] A similar effect is identified to be responsible for the thermochroism in polythiophenes.[30] Several DFT studies on isolated P(NDI2OD-T2) oligomers in the gas phase revealed a stable dihedral angle between the NDI part and the adjacent thiophene ring of around 40 to 47°,[31,32] which is reduced down to 34° upon aggregation.[19]

Reflection absorption IR spectroscopy (RAIRS or infrared reflection absorption spectroscopy IRRAS) experiments on preaggregated P(NDI2OD-T2) films by Giussani et al. yielded a dihedral angle of 38° in agreement with theoretical predictions.[33] This value, however, is deduced assuming that both thiophene rings of the T2 unit are lying flat on the substrate, and hence, is tantamount with the NDI unit's inclination relative to the substrate. Gann et al. used near edge X-ray absorption fine structure (NEXAFS) spectroscopy on a series of NDI copolymers with an increasing number of donor thiophene rings in order to separate the X-ray absorption pattern of the donor and acceptor units and to reveal structure-relevant information.[34] Different spectral signatures were successfully assigned to the distinct subunits in the monomer, but suffering from similar anisotropy of both components it was not possible to extract the dihedral angle and the molecular orientation with respect to the substrate.

To the best of our knowledge, it was yet not possible to separate the orientation of the NDI unit from that of the T2 part, when using X-ray scattering or NEXAFS for instance. Such measurements result in the mean orientation for the complete copolymer which makes is necessary to compare the spectroscopic data with simulation to deduce the orientation of the distinct subunits.[32,35] In contrast, RAIRS takes advantage of IR specificity that enables to derive the mean orientation of the different molecular building blocks (NDI and T2 units) forming the polymer chain, but suffers for the need of at least three differently prepared samples (one on a highly reflecting surface, one on a low reflecting one, and an isotropic sample), and hence, is limited in resolving transition moments which are orientated close the 0 or 90° relative to the substrate.[33]

In this study we prepared micrometer thin films of P(NDI2OD-T2) by spin-coating from CB or CN:Xyl solvents, what has been reported to result in supramolecular aggregates with different orientations of the $\pi-\pi$ stacking direction with respect to the substrate.[24] The structure of these films is then studied by transition moment orientational analysis (IR-TMOA): a technique based on the analysis of the absorption of structure specific bands depending on polarization *and* inclination of the incoming IR-light, to determine the three-dimensional orientation distribution of the molecular moieties.

MATERIALS AND METHODS

Sample Preparation. For preparing the samples P(NDI2OD-T2) (ActivInk N2200, Polyera Corp., USA) is dissolved under nitrogen atmosphere at a concentration of 35 g/L either in chlorobenzene (CB) or in a 1:1 chloronapthalene:xylene mixture (CN:Xyl) at 60 °C overnight. Afterward the films are spin coated for 30 s under nitrogen atmosphere at 1000 rpm on a 27.5′ wedge-shaped barium fluoride (BaF_2) IR window (Korth Kristalle GmbH, Kiel, Germany) to prevent interference effects arising from parallel surfaces and refractive index mismatch. Immediately after spin coating the samples are dried for 30 min in a vacuum oven. A part of them is measured either as such (film from CN:Xyl) or after subsequent annealing at 200 °C for 10 min inside the glovebox (films from CB and CN:Xyl). The distinct samples are labeled by the name of the used solvent and performed annealing (Table 1).

Infrared (IR) Measurements and Assignments. The infrared measurements are accomplished on a Bio-Rad FTS 6000 FTIR spectrometer. After the collimated and polarized IR beam passed through the sample film the transmitted radiation is measured with a spectral resolution of 2 cm^{-1} using a liquid nitrogen-cooled Mercury Cadmium Telluride (MCT) detector (Kolmar Technologies Inc., USA).

On the basis of the assignments elaborated by Giussani et al.[33] we identify the symmetric (ν_s) and antisymmatric C═O stretching vibrations (ν_{as}) located at the NDI unit, respectively termed a band at 1707 cm^{-1} and b band at 1667 cm^{-1}. Furthermore, we analyze the C−H out-of-plane bending vibration of the T2 unit (δ), termed c band

DOI: 10.1021/jacs.5b01755
J. Am. Chem. Soc. 2015, 137, 6034−6043

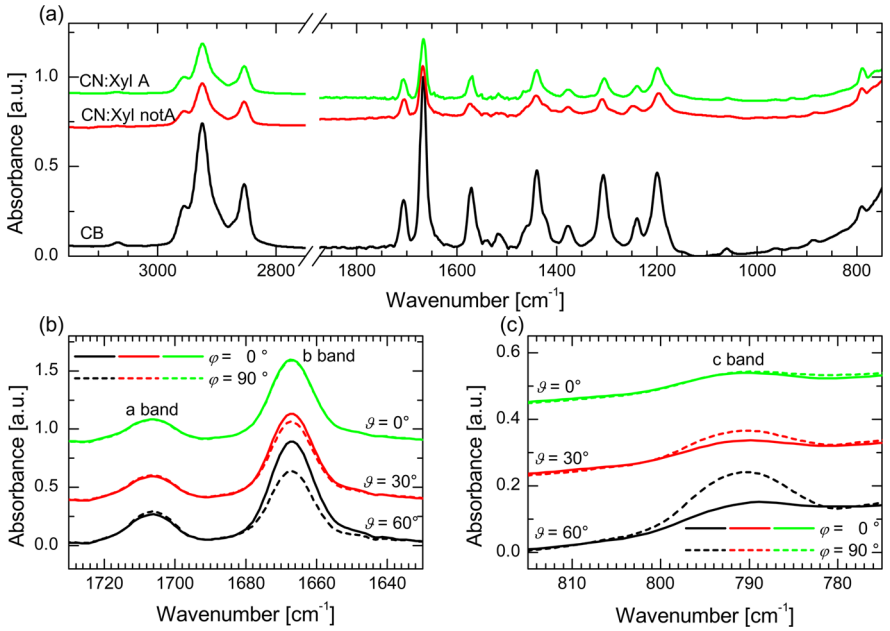

Figure 1. (a) Transmission FTIR spectra of the sample films CB, CN:Xyl notA, and CN:Xyl A. Panels (b) and (c) depict enlargements of orientation-relevant regions for sample CB. Note the polarization-dependent differences in absorption at high inclination representing preferred in-plane (b band) or out-of-plane orientation (c band) of the mean transition moment. For sake of clarity all spectra are shifted vertically.

at 791 cm^{-1} (Figure 1). Each vibration originates from a transition moment (TM, $\boldsymbol{\mu}$), that is well localized at one of these two respective structural units and exhibits a distinctive orientation with respect to the molecule (Figure 2b).[33] Therefore, we assign normalized vectors to the above-mentioned TMs, which can be described in the reference frame of the sample film by spherical coordinates: a polar angle Φ and an azimuthal angle Θ (Figure 2a). In particular, vector **a** refers to the TM of ν_s(C═O), **b** to ν_{as}(C═O) and c to δ(C−H).[33]

On the basis of these definitions, the orientation of the NDI- and T2-units can be calculated as follows: (1) The vector cross product (**a** × **b**) represents the NDI plane's normal vector (**n**), as **a** and **b** are both within the plane and perpendicular to each other. (2) The TM responsible for δ(C−H) is found at both thiophene rings and hence **c** represents the average orientation of the T2-unit. (Further discussion of the calculations can be found in the Supporting Information.)

Infrared Transition Moment Orientational Analysis (IR-TMOA). IR-TMOA is employed to evaluate the distribution of orientation of the molecular moieties based on the direction of IR active TMs.[36−39] To do so, spectra with the electric polarization, **E**, at an angle of φ = 0−180° are recorded for various orientations of the sample film with respect to the optical axis (ϑ = −60 to +60°). By that the projection of the sample's TMs onto the polarization plane is stepwise varied and measured (Figure 2a). Please note the difference between upper-case Θ and Φ representing the orientation of a TM in spherical coordinates with respect to the sample frame and lower-case ϑ and φ characterizing the direction of the IR beam with respect to film normal and the electric field polarization.

Because the integrated absorbance A (obtained through fitting a pseudo-Voigt function to each peak after the spectra were corrected for atmospheric water and a straight baseline was subtracted) for infinitely thin films is proportional to the molecular ensemble average (denoted as ⟨...⟩) over the scalar product $(\boldsymbol{\mu}\cdot\mathbf{E})^2$,

$$A \propto \langle(\boldsymbol{\mu}\cdot\mathbf{E})^2\rangle \tag{1a}$$

the current polarization and inclination directly affect the amount of absorbed light. Furthermore, eq 1a can be expressed as

$$A \propto \mathbf{E}^{\mathrm{T}}\cdot\underline{\mu}\cdot\mathbf{E} \tag{1b}$$

where $\underline{\mu}$ represents a matrix defined through $\underline{\mu}_{ab} = \langle\mu_a\mu_b\rangle$ with $a,b \in [x,y,z]$. Since $\underline{\mu}$ is a symmetric matrix in the reference frame of the sample coordinate system, it can be diagonalized resulting in a new matrix $\underline{\mu}'$ with A_i, A_j, and A_k (the eigenvalues of $\underline{\mu}$) on the main diagonal. That diagonalization represents a transformation from the sample coordinate (x,y,z) into the principal axes system (i,j,k) of the absorption tensor. The relative orientation of this two coordinate systems is described by three Euler angles α, β, and γ in ZXZ convention. Thus, through fitting $\underline{\mu}$ to the measured absorbance pattern, which depends on ϑ and φ, we determine the degree of alignment (eigenvalues A_i, A_j, A_k) with the principal axes of absorption (eigenvectors **i**, **j**, **k**) and their particular orientation (Euler angles α, β, γ) with respect to the sample coordinate system.

An equivalent but more common description of the mentioned "degree of alignment" (A_i) is the molecular order parameter along the principal directions of the orientation distribution.[39,40] For direction **i** it reads:

$$S_{ii} = \frac{1}{2}\left(\frac{3\mu'_{ii}}{\sum_m \mu'_{mm}} - 1\right) \tag{2}$$

with $m \in [i,j,k]$. S_{jj} and S_{kk} are defined analogously. This equation equals 1 when all TMs are aligned along the corresponding axis, −1/2 when all TMs are perpendicular to it, or 0 in the isotropic case.

RESULTS

Molecular Orientation of Sample CB. At a normal incidence (ϑ = 0), no significant differences can be seen between the recorded FTIR spectra for the differently prepared samples (Figure 1a) and for all polarization angles (Figure 1b and c). Different peak heights are arising from the varying film thicknesses.

In case sample CB is inclined it becomes evident that the absorbance of all three aforementioned vibrations depends on the polarization φ: For $|\vartheta| > 0°$, δ(C−H) and ν_s(C═O) absorb strongest, respectively more, at φ = 90° (p-polarization), whereas ν_{as}(C═O) does so at φ = 0 or 180° (s-polarization) (Figure 1b and c). This already demonstrates differently oriented TMs. Two exemplary cases of the polarization- and inclination-dependent absorbance pattern shall be given here: (1) When the light is s-polarized (φ = 0 or 180°), **E** is oscillating parallel to the rotation axis of inclination (cf.

DOI: 10.1021/jacs.5b01755
J. Am. Chem. Soc. 2015, 137, 6034−6043

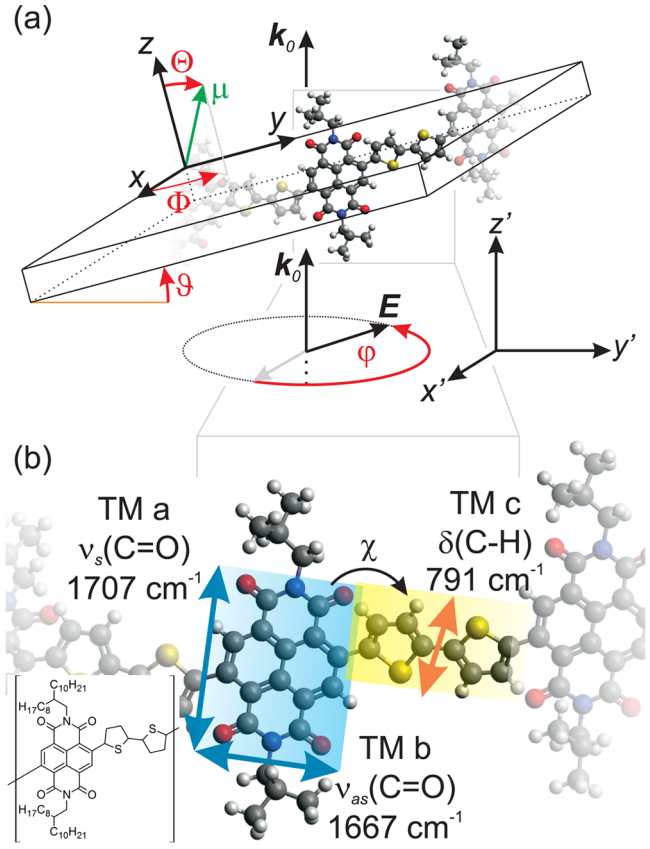

Figure 2. (a) Scheme of the sample geometry for IR transition moment orientational analysis (IR-TMOA). The incident IR light ($\mathbf{k}_0$) is propagating along the z' direction with the electric field polarized within the $x'y'$ plane. The sample coordinate system (x,y,z) is inclined relative to the laboratory frame (x',y',z') while the polarization (φ)- and inclination (ϑ)-dependent absorbance is measured. By that, the full molecular order parameter tensor with respect to the sample coordinate system for the individual (IR-specific) transition moments can be deduced. (b) Schematic representation of a sample fragment along with the transition moments (arrows) used to evaluate the molecular structure. The planar NDI and T2 units are indicated in blue and yellow, respectively. For sake of clarity the C_8H_{17} and $C_{10}H_{21}$ alkyl side chains are replaced by methyl groups; the inset depicts the chemical structure of P(NDI2OD-T2).

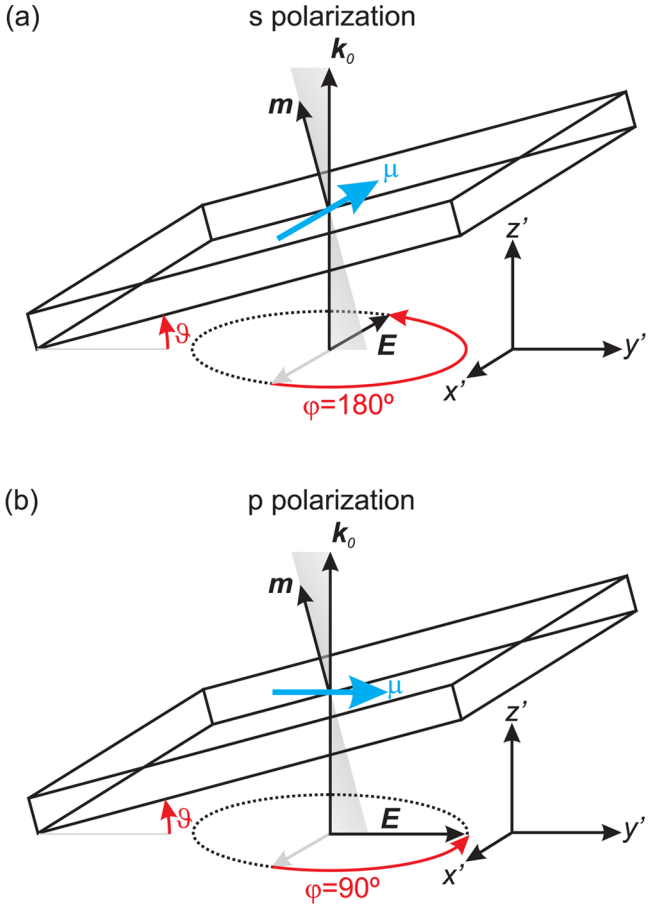

Figure 3. Scheme illustrating the particular cases of s and p polarization. (a) At a polar angle of φ = 0 or 180° the electric field vector **E** runs parallel to the axis of inclination x', and hence, perpendicular to the plane of incidence spanned between the film's normal vector **m** and the light path $\mathbf{k}_0$ (light gray). In that case only the component of the TM $\boldsymbol{\mu}$ in parallel to the film is probed independent of inclination. (b) For a polar angle of φ = 90° **E** vibrates within the plane of incidence. Thus, a component of the TM pointing out of the sample film can be detected.

Figure 3a). Consequently, at this polarization components of the TMs parallel to the substrate are probed irrespective of the particular inclination. This is only correct in case the eigenvectors are located within the film plane, which is, indeed, valid for our samples as shown later. (2) In contrast, when the light is p-polarized (φ = 90°), **E** is oscillating within the plane of incidence and pointing out of the film by an angle depending on the inclination. Thus, components of the TMs perpendicular to the film are probed, which are not accessible in polarization-dependent IR measurements at normal incidence (ϑ = 0°).[41]

For sample CB, one finds a preferred alignment of **a** (TM of ν_s(C═O), Figure 2b, Figure 4) perpendicular to the sample plane (S_{zz} = 0.10 ± 0.01), whereas **b** (TM of ν_{as}(C═O)) is oriented mainly parallel to it (S_{zz} = −0.33 ± 0.01). This already indicates that the NDI unit is tilted with respect to the substrate. The average normal vector of the T2 unit (**c**) on the other hand is again aligned perpendicularly (S_{zz} = 0.65 ± 0.02), meaning that the T2 planes exhibits a *face on* orientation.

The vanishing dichroism at normal incidence proves an uniaxial distribution (rotationally symmteric) of the TMs with respect to the sample film's normal vector (**z**). This is further verified through the quantitative analysis of IR-TMOA. In particular we find for all samples $\beta \leq 3°$, representing the deviation of the principal axis k from z. This is smaller than the experimental uncertainty, and thus, we identify k with z meaning, respectively β = 0°. From that it follows directly that the other two axes (i and j) have to be located within the xy plane. We find $A_i \approx A_j$ (fits displayed in Figure 4 and parameters in Table 2), hence justifying rotational symmetry with respect to k (= z) and approving $i = x$ and $j = y$.

Inquiring for the molecular structure we have to consider the following: Rivnay et al. demonstrated that the aggregated chains in films of P(NDI2OD-T2) treated below the melting temperature adopt a face-on arrangement in which the chain backbone units orient preferentially parallel to the substrate.[14,15] In this model the π−π stacking takes place mainly perpendicular to the film plane (see Figure 3 in ref 14). Recently, Steyrleuthner et al. derived the coherence length of aggregated chains being 5 times larger in the direction parallel to substrate than perpendicular to it.[24] Supplementary to that,

DOI: 10.1021/jacs.5b01755
J. Am. Chem. Soc. 2015, 137, 6034−6043

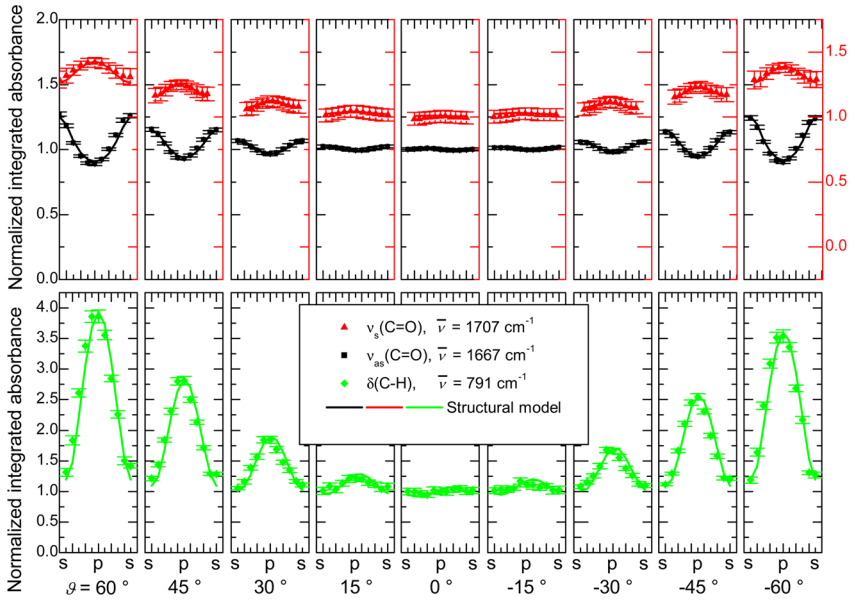

Figure 4. Integrated absorbance of ν_s(C═O), ν_{as}(C═O), and δ(C−H) of sample CB depending on inclination (ϑ) and polarization (p: electric field vector parallel to the plane of incidence at φ = 90°; s: perpendicular at φ = 0 or 180°). The solid lines represent the absorbance pattern, which results from the structural model using the parameters as denoted in Table 2. For sake of clarity and comparability all values are normalized to the mean absorbance at normal incidence (ϑ = 0°). The scales on the left and the right-hand side in the upper part are shifted but equal in size, whereas the scale in the lower part is as twice as large as those in the upper one.

Table 2. Relevant Parameters of the Structural Model Derived from the Integrated Absorbance Depending on Inclination and Polarization of Sample CB[a]

quantity	ν_s(C═O)	ν_{as}(C═O)	δ(C−H)
A_i	2.79	13.55	0.52
A_j	2.80	13.37	0.44
A_k	3.67	3.35	3.14

[a]The values A_i, A_j, and A_k denote the absorbance according to the principal axes (i,j,k). Because the absorption is isotropic with respect to the film plane ($A_i \approx A_j$ and $\beta \leq 3°$), we identify the principle axis system with the sample coordinate system. The full parameter set including the Euler angles α, β, and γ, and the refractive index of the sample material n are given in Table S1 in the Supporting Information.

Schuettfort et al. observed a 41°-tilt of the mean signal from the chain backbone units in bulk with regard to the substrate.[35] In accord with these findings we propose a laterally extended planar structure of aggregates being comprised of tilted NDI and T2 units. That allows for the use of a single azimuthal angle representing the orientation of a TM or a plane normal vector to describe the molecular structure. Considering the rotationally symmetric absorbance pattern we introduce a cone with its symmetry axis parallel to z and all TMs equally distributed on its lateral surface (Figure 5a). The opening angle Θ of that cone corresponds to the azimuthal angle and is determined through the ratio $A_z/A_\parallel$

$$\cos(\Theta) = \sqrt{\frac{A_z}{A_z + 2A_\parallel}} \quad (3)$$

where $A_\parallel = (A_x + A_y)/2$ represents the absorbance with regard to any direction within the xy plane, and differs for the different TMs.[41]

In the framework of the this model the TM **a** exhibits an angle of 39° relative to the substrate (Θ = 51°), while **b** features an angle of 19° to it (Θ = 71°). The resulting normal vector of the NDI plane is tilted 45° away from the substrate normal, which is tantamount to the inclination of the NDI plane out of the film. **c** is tilted by Θ = 29° relative to the film normal, meaning that the T2 plane shows an inclination of 29° with respect to the substrate (*face on* orientation). A graphical representation can be found in Figures 5 and 7 and all parameters of orientation resulting from the model in Table 3.

We determine the angle between the NDI and T2 plane based on their particular inclinations. Two possible cases can be constructed: (1) The NDI unit is rotated in one direction around the polymer backbone; the T2 part is turned in the opposite way. Then the planes' cutting angle χ would amount to 74° (45° + 29°). (2) Both parts are rotated in the same direction. Then the angle between the planes would be 16° (45° − 29°). Unfortunately, these two variants cannot be distinguished. Additionally, the cutting angle between the NDI and T2 plane χ, as discussed here, can be different from the dihedral angle, as derived from simulations for instance. Since the former is defined through the relative orientation of the NDI plane to the T2 plane (which is the mean of the two thiophene ring planes in the T2 unit), whereas the latter originates from atomic bonds between the NDI part and the first adjacent thiophene ring, a torsion between the two rings gives rise to a deviation of the normal vector of the adjacent ring from that of the T2 plane. Thus, the cutting angle and the dihedral angle differs by half of the torsion (cf. Figure S1 in the Supporting Information).

Molecular Orientation of Samples CN:Xyl. The TMs related to the NDI-units show qualitatively the same orientational distribution as the CB-sample but a weaker ordering (Tables 3 and S4 in the Supporting Information). The absorbance of δ(C−H) on the other hand displays a distinct maximum for s-polarized light (Figure 6) demonstrating that the mean TM of the aromatic T2 units (**c**) orients preferentially parallel to the substrate. Consequently, the T2 plane has to feature an *edge on* orientation. This is contrary to the case of

DOI: 10.1021/jacs.5b01755
J. Am. Chem. Soc. 2015, 137, 6034−6043

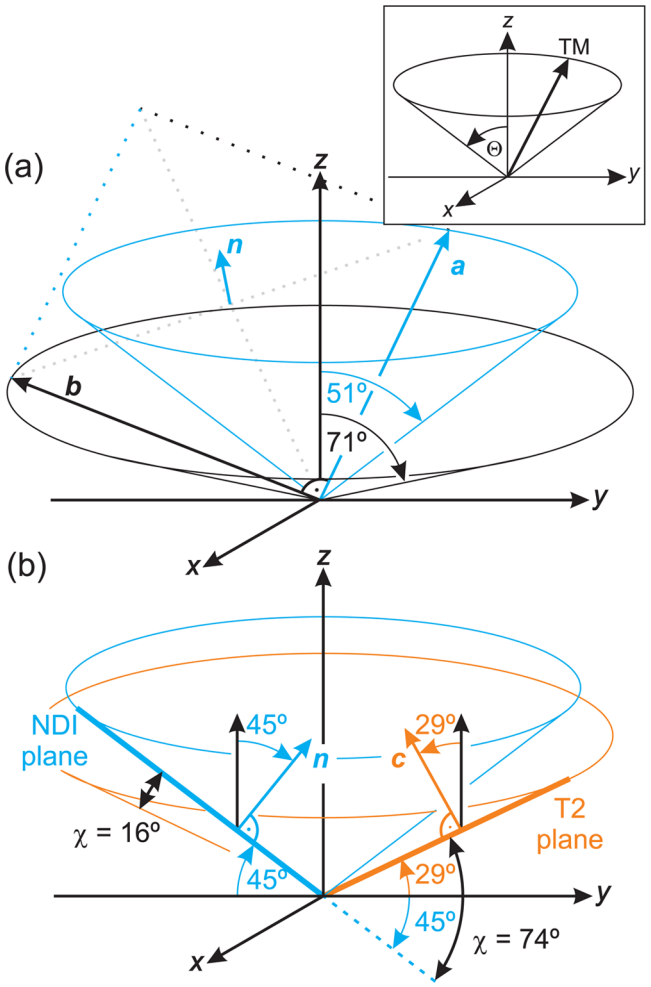

Figure 5. Illustration of the rotationally symmetric distributions of the TMs for the example of sample CB. (a) The TMs **a** (blue) and **b** (black) are located at the according cone's lateral surface, while they are orthogonal with respect to each other. Their vector cross product gives the NDI plane's normal vector **n**. The term opening angle, which is identical to the TM's orientation Θ, is used as depicted in the inset. (b) Two cones representing the inclination of the NDI and the T2 plane, respectively the NDI plane's normal vector and the TM **c**. When the NDI and the T2 plane are tilted in opposite directions around the polymer backbone (*x* axis) the cutting angle χ results from the sum of the particular inclinations (74°, case 1). If both planes are rotated in the same direction, χ is given by the difference of the planes' inclination (16°, case 2).

CB, where a distinct *face on* orientation is deduced based on the inverted dependence of absorbance on polarization (Figure 6, and the corresponding order parameters in Table S4 in the Supporting Information).

The influence of annealing on the mean orientation directions is negligible; β changes from 0.0, 2.3, and 1.8° (Table S2 in the Supporting Information) to 1.4, 0.2, and 1.0° (Table S3). These variations in the Euler angles are smaller compared to the measurement uncertainty (5°). In contrast, an increase of the order parameters is found: S_{zz} for **a** and **c** changes from 0.03 and −0.23 to 0.11 and −0.32 (Table S4), respectively. Rotational symmetry with respect to the film normal is preserved for all samples and therefore our model can be applied as well (Tables S2 and S3 in the Supporting Information).

Table 3. Geometrical Orientation of the TMs a, b, and c Corresponding to ν_s(C═O), ν_{as}(C═O), and δ(C−H), and of the Normal Vector of the NDI Plane n in the Framework of Our Model[a]

sample		a	b	n (NDI)	c (T2)	χ[°]
CB	Θ/°	51	71	45	29	16/74
	Φ/°	−107	0	70	–	–
Cn:Xyl notA	Θ/°	53	63	49	65	16/114(66)
	Φ/°	−112	0	63	–	–
CN:xyl A	Θ/°	51	63	52	70	18/122(58)
	Φ/°	−115	0	66	–	–

[a]Please note that without loss of generality we set $\Phi_b = 0$ and calculate Φ_a (cf. Supporting Information). Because of geometrical reasons, there exist two symmetric and exact values of $\pm\Phi_a$, which are coequal. Consequently, the polarization of the NDI plane has also two possible values $\pm\Phi_{NDI}$ of equal rank. For simplicity we choose one possibility. The planes' cutting angle χ gives the difference/sum of the inclination of the NDI and T2 planes. The angles are accurate up to ±5°. (The corresponding order parameters for the different TMs (S_{ii},S_{jj},S_{kk}) are provided in Table S4 in the Supporting Information.)

For sample CN:Xyl notA the TM **a** exhibits an angle of 37° with respect to the substrate (Θ = 53°) being similar to sample CB. **b** (S_{zz}=−0.19 ± 0.01) is tilted by about 27° out of the substrate plane (Θ = 63°) pointing slightly more upright than in CB (Θ = 71°). Thus, the NDI unit is inclined by about 49° with respect to the substrate (Table 3). Annealing results in changes of the azimuthal angles of less than 3° for NDI and are therefore neglected in the discussion of the model. The absorbance pattern of the T2 plane reveals an inclination of 65° prior annealing and 70° afterward. The planes' cutting angle χ is determined to be 114°, respectively 66° (180° − 114°), for case 1 and 16° for case 2 prior annealing (Table 3). Afterward 122°, respectively 58° (180° − 122°), for case 1 and 18° for case 2 are found.

DISCUSSION

Solvent is proven to be of fundamental importance for the sample structure: Using chlorobenzene the T2 plane orients preferentially parallel to the substrate with an angle of inclination of 29°. The NDI plane instead is inclined by 45° (TM **a** by 39° and TM **b** by 19°). In case the solvent is exchanged through a 1:1 chloronaphthalene:xylene mixture, the NDI unit basically retains its inclination (Θ = 49° before and 52° after annealing), whereas the T2 part undergoes a remarkable reorientation from a *face on* into an *edge on* alignment (Θ = 65° before annealing and 70° afterward). All three films provide evidence of partialy aggregated chains as indicated by UV−vis absorption spectroscopy (cf. Figure S3 in the Supporting Information).[24]

Recently, Giussani et al.[33] combined normal incidence and reflection−absorption IR spectroscopy (RAIRS) to derive the molecular orientation of P(NDI2OD-T2) spin-coated from a chlorobenzene solution. They obtained that the NDI plane is inclined by 38°, respectively 142°, relative to the substrate, under the assumption that the TM **b** runs parallel to it.[14,15,33] Consequently, the NDI unit's inclination depends only on the tilt of the TM **a**. Using IR-TMOA we determine a similar angle for the TM **a** (39°); the deviated inclination of the NDI part arises from the tilt of the TM **b**. Having a close look at Figure 4 in ref 33, it is evident that the b band absorbs light in case of RAIRS. This, indeed, indicates a deviation from the performed

DOI: 10.1021/jacs.5b01755
J. Am. Chem. Soc. 2015, 137, 6034−6043

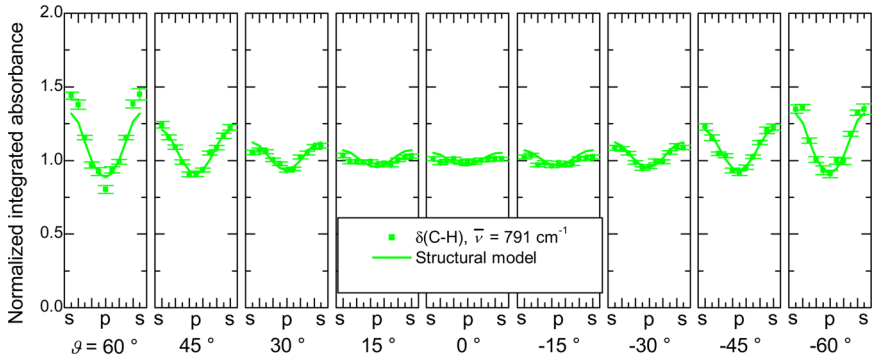

Figure 6. Integrated absorbance of δ(C−H) of sample CN:Xyl A depending on inclination (ϑ) and polarization (p: electric field vector parallel to the plane of incidence; s: perpendicular). The solid lines represent the absorbance pattern, which results from the structural model using the parameters as denoted in Table S3 (in the Supporting Information). In contrast to sample CB (Figure 4) an s-polarization is evident indicating an in-plane orientation of the TM, and hence, an edge on orientation of the T2 plane. For the sake of comparability all values are normalized to the mean absorbance at normal incidence (ϑ = 0°).

assumption. Because the TM **b** is not parallel to the substrate, but in our case inclined by 19°, the overall tilt of the NDI unit rises to 45°.

In addition, Giussani et al.[33] assumed the orientation of the T2 part to be parallel to the substrate. In contrast, we unambiguously find that the T2 plane is inclined, as well. Its tilt angle can be determined to be 29°. As in case of the NDI part discussed before, Figure 4 in ref 33 clearly shows an absorption of the c band for normal incidence (transmission), which would not be the case when all TMs **c** were fully perpendicular to the substrate.

Simulations addressing the molecular structure revealed a dihedral angle of ±138°, respectively ±42°, between NDI and the adjacent thiophene ring assuming a torsion angle between both thiophene rings of ±148°.[33] Hence, the normal vector of each of that two thiophene rings is inclined by +16 or −16° relative to the mean T2 normal vector (**c**) that we obtain from IR-TMOA (Figure S1 in the Supporting Information). Consequently, the cutting angle, should deviate by 16° from the dihedral angle. This is fairly the case with regard to Giussani et al.[33] and with other studies performed by Schuettfort et al.[32] However, assuming that the TM **b** would run parallel to the substrate and TM **c** perpendicular to it (with all thiophene rings parallel to the substrate and no torsion between them), then the cutting and dihedral angle would coincide. In that case they amount to 39° being in accord with recently published data.[33]

In addition, Giussani et al. found that the polymer backbone, which is believed to be identical to the axis of rotation of the distinct planes, is turned by 23° relative to the direction of TM **b**.[33] On the basis of that, we calculate possible values of the planes' cutting angle χ depending not only on the inclination of the planes Θ, but also on their polarization angles Φ. Because the absorption shows rotational symmetry, we use the inclination angles as derived from the spectroscopic measurement and take the difference of the polar angles $\Delta\Phi = \Phi_{NDI} - \Phi_{T2}$ (cf. Figure S2 in the Supporting Information). As discussed previously $\Delta\Phi$ = 180° corresponds to case 1 with χ = 74°, whereas $\Delta\Phi$ = 0° matches case 2 with χ = 16° for sample CB. Because both parts, the NDI as well as the T2 unit, are aromatic structures, and hence, planar and rather stiff, we believe a difference in their polar angles $\Delta\Phi$ > 30° is not reasonable. In that limit, χ is reduced to 72° for case 1 or increased to 24° for case 2.

Recently, Schuettfort et al. performed near-edge X-ray absorption fine-structure (NEXAFS) spectroscopy on similar films spin-coated from a chlorobenzene solution on silicon wafers.[35] A mean inclination of 41° has been found, but it was not possible to separate the signals from the NDI and T2 units. Assuming the π−π stacking proceeds perpendicular to the substrate, they conclude it is more probable that the NDI part, on which the side chains are tethered, is oriented more parallel to the substrate. They use a dihedral angle of 47° from a simulation and calculated that the NDI part is by 16.5° (35% of the dihedral angle) less inclined than the mean signal. Consequently, the smaller T2 unit then has to be tilted by 30.5° (65% of the dihedral angle) more upright compared to the mean. Please note that in this particular experiment the molecular orientation is described by the mean normal vector of the aromatic rings, similar to the mean normal vectors of atomic planes used in this work. When separating the orientation of the NDI and the T2 units the angle discussed is adequately described (in the terminology of this article) by cutting angle, rather than dihedral angle (see discussion above). For our samples prepared from a chlorobenzene solution we find that the T2 plane is orientated preferentially parallel to the substrate and that the NDI part is tilted more upright. Assuming a cutting angle of 16° as discussed above, a 35% deviation from that would amount to 5.6°, a 65% deviation to 10.4°. Consequently, a mean signal at 41° inclination would correspond to an orientation of the NDI part of 47° (41° + 6°) and of the T2 part of 31° (41° − 10°) being in agreement with our findings of 45°, respectively 29°.

Steyrleuthner et al. prepared films using both solvents, chlorobenzene and a chloronaphthalene:xylol mixture, and performed grazing-incidence X-ray diffraction (GIXD) on those. They found that in case of CB, the π−π stacking proceeds perpendicular to the substrate, whereas for CN:Xyl the stacking direction runs parallel to the surface.[24] This results are in direct correlation with our findings: For sample CB the T2 plane is oriented preferentially parallel to the substrate and so the mean polymer orientation (NDI and T2), too. In that case π−π stacking perpendicular to the substrate is favored. In contrast, for the samples CN:Xyl notA and CN:Xyl A the T2 plane is oriented preferentially perpendicular to the substrate, while the NDI part retains essentially unaffected. Thus, the mean alignment of the molecular planes is preferentially perpendicular to the substrate and the π−π stacking proceeds

DOI: 10.1021/jacs.5b01755
J. Am. Chem. Soc. 2015, 137, 6034−6043

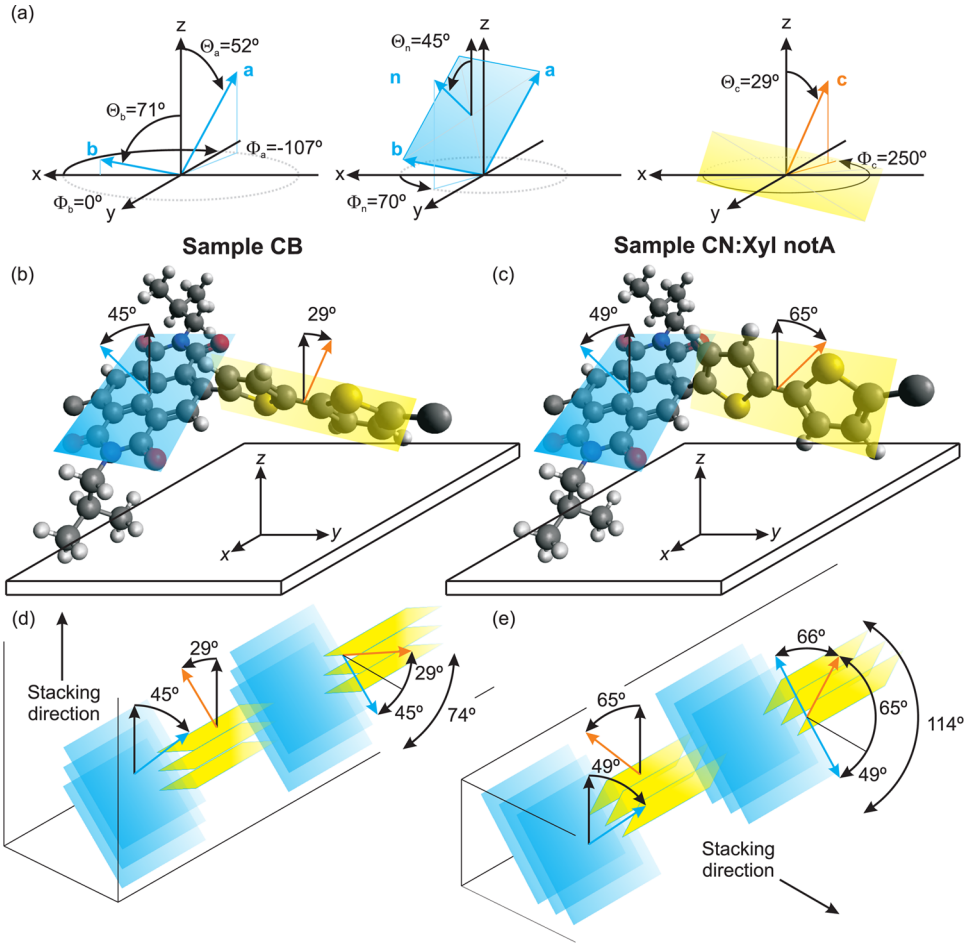

Figure 7. (a) Scheme of the microscopic orientation of the molecular planes as experimentally deduced by IR-TMOA for case 1 (NDI and T2 plane rotate in opposite directions). The NDI plane (blue), respectively its normal vector **n**, is defined through the TMs **a** and **b**, whereas the TM **c** represents the normal vector of the T2 plane (yellow). Its polarization Φ_c is set in accord to case 1 ($\Phi_c = 180° + \Phi_n$). (b) When prepared using chlorobenzene (sample CB), the NDI unit is inclined by 45° relative to the substrate, whereas the T2 part (yellow) features an angle of 29° and a *face on* orientation. (c) Using a chloronaphthalene:xylene mixture (sample CN:Xyl notA) results in a distinct *edge on* orientation of the T2 unit (Θ_c = 65°, 70° for sample CN:Xyl A). The NDI block, instead, retains its alignment (Θ = 49°, 52° for CN:Xyl A). For sake of clarity the C_8H_{17} and $C_{10}H_{21}$ alkyl chains are replaced by methyl groups. (d,e) Illustrated interpretation of the distinct $\pi-\pi$ stacking behavior: Following the orientation of the T2 unit and the NDI-T2 planes' cutting angle the lamellae are formed either perpendicular to the substrate (d) or parallel to it (e). Please note the turned coordinate system in panel (a), which provides the visualization of the derived parameters (Table 3), compared to the others, that gives an impression of the molecular structure. Because of the rotational symmetry both variants are coequal.

parallel to it. One has to keep in mind that X-ray scattering detects periodic electron density features. Thus, neither the NDI nor the T2 plane have to be strictly aligned perpendicular to the direction of stacking.

The effect of the solvents could possibly be explained as follows: While sample CB dries within 1 min, the CN:Xyl samples needs considerably longer (30 min). Thus, such distinct stacking kinetics of preaggregates already present in the solution[19,24] give rise to different (semi)stable conformations. An indication for this is provided by the frequently observed reorientation of CB samples from a face on alignment as a result of spin-coating into an edge on structure when heated above the melting temperature.[33] In addition, chloronaphthalene shields the aromatic structures of the sample polymer from interacting with themselves, the substrate, or the air boundary, because of its polarizability, and the aliphatic side chains arrange at the interfaces. Since the domains are highly interconnected,[24] the beginning chain stacking (likely at the boundaries) is permeated throughout the whole sample. Please bear in mind that, so far, we are characterizing such films. Motivated through the solvent-dependent direction of the $\pi-\pi$ stacking, as reported,[24] we ascertain the impact of the different solvents to the T2 unit, while the NDI part is basically unaffected. The elucidation of the underlying mechanism remains for future prospects.

With regard on the planes' cutting angle we see a slight annealing effect on the orientation of both planes (aligning more upright), the anticipated strong impact on the IR-sensitive molecular structure as implied through the change in the UV–vis absorption pattern (see Figure 2 in ref 24 and Figure S3 in the Supporting Information) is missing. However, as a consequence of the thermal treatment the molecular order parameter increases for the TMs **a** and **c**, but does not reach the value of sample CB in case of the TM **b** (Table S4 in the Supporting Information). These findings suggest a relaxation into a more ordered structure at temperatures below the melting point and are in agreement with an increase in the aggregation content, structural correlation lengths and charge mobility as a result of annealing.[24]

DOI: 10.1021/jacs.5b01755
J. Am. Chem. Soc. 2015, 137, 6034–6043

CONCLUSION

On the basis of molecular vibrations information on the structure of spin-coated films of P(NDI2OD-T2) are deduced. By means of the method of transition moment orientational analysis (IR-TMOA) and assignments elaborated by Giussani et al.[33] a refined structural model is proposed for samples prepared from a chlorobenzene (CB) solution or a 1:1 chloronaphthalene:xylene mixture (CN:Xyl). In particular it is demonstrated that in case of CB the T2 units orient preferentially flat to the substrate (*face on*) exhibiting an inclination of 29°. The NDI unit instead is inclined by 45° (Figure 7). The transition moments (TMs) which define the planes of the NDI or the T2 unit are distributed in a rotationally symmetric fashion. Thus, macroscopic anisotropy parallel to the substrate is absent, but prevails perpendicular to it.

Exchanging CB through CN:Xyl as solvent hardly affects the orientation of the NDI unit (inclination of 49° or 52°), while the T2 part undergoes a remarkable transition from a distinct *face on* into an *edge on* orientation (from 29° to 65° or 70° inclination, Figure 7). The reorientation of that specific unit gives rise to a change in the overall polymer backbone orientation and an altered π-π stacking direction relative to the substrate as evident in scattering experiments.[24] Through the choice of the particular solvent the stacking direction, and hence, the orientation of the side chains can be adjusted, though the mean alignment of the NDI part, on which the side chains are tethered, is retained. This demonstrates the need for examining the orientation of all parts of the polymer chain to understand its structure formation and to tailor it for application-specific demands.

The cutting angles between the NDI and mean T2 plane are determined for all samples to be between 16 and 18° assuming that both planes rotate in the same direction around the polymer backbone. In case the planes turn in opposite ways values of 74, 114, or 122° are derived for sample CB, CN:Xyl notA, and CN:Xyl A, respectively. During annealing both planes align more upright, but the anticipated strong impact on the cutting angle has not been found. Furthermore, the thermal treatment causes an increase of the molecular order parameter, which represents a relaxation of the molecular arrangement at temperatures below the polymer's melting point in accord with an increase in crystallinity, structural correlation lengths and charge mobility.[24]

ASSOCIATED CONTENT

Supporting Information

The complete set of parameters of the absorption tensor (Euler angles and eigenvalues) for all the different samples, the geometrical orientation of the probed moieties (including order parameters), as well as details of the geometry of the absorption pattern and the calculation of the NDI plane's normal vector are provided. The Supporting Information is available free of charge on the ACS Publications website at DOI: 10.1021/jacs.5b01755.

AUTHOR INFORMATION

Corresponding Author

*anton@physik.uni-leipzig.de

Notes

The authors declare no competing financial interest.

ACKNOWLEDGMENTS

We thank Zhihua Chen and Antonio Facchetti (Polyera Corporation, USA) for supplying the P(NDI2OD-T2). Financial support by the Deutsche Forschungsgemeinschaft (DFG, Project B5 within SFB/TRR 102 "Polymers under multiple constraints: restricted and controlled molecular order and mobility"), through the Leipzig School of Natural Sciences "Building with Molecules and Nano-Objects" (BuildMoNa), by the Sächsische Forschergruppe FOR 877 "From Local Constraints to Macroscopic Transport", and by the Helmholtz Association (Helmholtz-Energie-Allianz "Hybrid-Photovoltaik") is highly acknowledged.

REFERENCES

(1) Sirringhaus, H. *Adv. Mater.* **2014**, *26*, 1319−1335.
(2) Olivier, Y.; Niedzialek, D.; Lemaur, V.; Pisula, W.; Müllen, K.; Koldemir, U.; Reynolds, J. R.; Lazzaroni, R.; Cornil, J.; Beljonne, D. *Adv. Mater.* **2014**, *26*, 2119−2136.
(3) Rivnay, J.; Mannsfeld, S. C. B.; Miller, C. E.; Salleo, A.; Toney, M. F. *Chem. Rev.* **2012**, *112*, 5488−5519. PMID: 22877516
(4) Yan, H.; Chen, Z.; Zheng, Y.; Newman, C.; Quinn, J. R.; Dotz, F.; Kastler, M.; Facchetti, A. *Nature* **2009**, *457*, 679−686.
(5) Steyrleuthner, R.; Schubert, M.; Jaiser, F.; Blakesley, J. C.; Chen, Z.; Facchetti, A.; Neher, D. *Adv. Mater.* **2010**, *22*, 2799−2803.
(6) Moore, J. R.; Albert-Seifried, S.; Rao, A.; Massip, S.; Watts, B.; Morgan, D. J.; Friend, R. H.; McNeill, C. R.; Sirringhaus, H. *Adv. Energy Mater.* **2011**, *1*, 1614−6840.
(7) Schubert, M.; Dolfen, D.; Frisch, J.; Roland, S.; Steyrleuthner, R.; Stiller, B.; Chen, Z.; Scherf, U.; Koch, N.; Facchetti, A.; Neher, D. *Adv. Energy Mater.* **2012**, *2*, 369−380.
(8) Fabiano, S.; Chen, Z.; Vahedi, S.; Facchetti, A.; Pignataro, B.; Loi, M. A. J. *J. Mater. Chem.* **2011**, *21*, 5891−5896.
(9) Tang, Y.; McNeill, C. R. *J. Polym. Sci., Part B: Polym. Phys.* **2013**, *51*, 403−409.
(10) Zhou, N.; Lin, H.; Lou, S. J.; Yu, X.; Guo, P.; Manley, E. F.; Loser, S.; Hartnett, P.; Huang, H.; Wasielewski, M. R.; Chen, L. X.; Chang, R. P. H.; Facchetti, A.; Marks, T. J. *Adv. Energy Mater.* **2014**, *4*, 1300785.
(11) Schubert, M.; Collins, B. A.; Mangold, H.; Howard, I. A.; Schindler, W.; Vandewal, K.; Roland, S.; Behrends, J.; Kraffert, F.; Steyrleuthner, R.; Chen, Z.; Fostiropoulos, K.; Bittl, R.; Salleo, A.; Facchetti, A.; Laquai, F.; Ade, H. W.; Neher, D. *Adv. Funct. Mater.* **2014**, *24*, 4068−4081.
(12) Mori, D.; Benten, H.; Okada, I.; Ohkita, H.; Ito, S. *Adv. Energy Mater.* **2014**, *4*, 1301006.
(13) Mori, D.; Benten, H.; Okada, I.; Ohkita, H.; Ito, S. *Energy Environ. Sci.* **2014**, *7*, 2939−2943.
(14) Rivnay, J.; Toney, M. F.; Zheng, Y.; Kauvar, I. V.; Chen, Z.; Wagner, V.; Facchetti, A.; Salleo, A. *Adv. Mater.* **2010**, *22*, 4359−4363.
(15) Rivnay, J.; Steyrleuthner, R.; Jimison, L. H.; Casadei, A.; Chen, Z.; Toney, M. F.; Facchetti, A.; Neher, D.; Salleo, A. *Macromolecules* **2011**, *44*, 5246−5255.
(16) Takacs, C. J.; Treat, N. D.; Krämer, S.; Chen, Z.; Facchetti, A.; Chabinyc, M. L.; Heeger, A. J. *Nano Lett.* **2013**, *13*, 2522−2527.
(17) Sciascia, C.; Martino, N.; Schuettfort, T.; Watts, B.; Grancini, G.; Antognazza, M. R.; Zavelani-Rossi, M.; McNeill, C. R.; Caironi, M. *Adv. Mater.* **2011**, *23*, 5086−5090.
(18) Luzio, A.; Criante, L.; D'Innocenzo, V.; Caironi, M. *Sci. Rep.* **2013**, 3425.
(19) Steyrleuthner, R.; Schubert, M.; Howard, I.; Klaumünzer, B.; Schilling, K.; Chen, Z.; Saalfrank, P.; Laquai, F.; Facchetti, A.; Neher, D. *J. Am. Chem. Soc.* **2012**, *134*, 18303−18317.
(20) Caironi, M.; Bird, M.; Fazzi, D.; Chen, Z.; Di Pietro, R.; Newman, C.; Facchetti, A.; Sirringhaus, H. *Adv. Funct. Mater.* **2011**, *21*, 3371−3381.
(21) Lange, I.; Blakesley, J. C.; Frisch, J.; Vollmer, A.; Koch, N.; Neher, D. *Phys. Rev. Lett.* **2011**, *106*, 216402.

DOI: 10.1021/jacs.5b01755
J. Am. Chem. Soc. 2015, 137, 6034−6043

(22) Tremel, K.; Fischer, F. S. U.; Kayunkid, N.; Pietro, R. D.; Tkachov, R.; Kiriy, A.; Neher, D.; Ludwigs, S.; Brinkmann, M. *Adv. Energy Mater.* **2014**, *4*, 1301659.
(23) Fabiano, S.; Himmelberger, S.; Drees, M.; Chen, Z.; Altamimi, R. M.; Salleo, A.; Loi, M. A.; Facchetti, A. *Adv. Energy Mater.* **2014**, 1301409.
(24) Steyrleuthner, R.; di Pietro, R.; Collins, B. A.; Polzer, F.; Himmelberger, S.; Schubert, M.; Chen, Z.; Zhang, S.; Salleo, A.; Ade, H.; Facchetti, A.; Neher, D. *J. Am. Chem. Soc.* **2014**, *136*, 4245−4256.
(25) Fazzi, D.; Caironi, M.; Castiglioni, C. *J. Am. Chem. Soc.* **2011**, *133*, 19056−19059.
(26) Donley, C. L.; Zaumseil, J.; Andreasen, J. W.; Nielsen, M. M.; Sirringhaus, H.; Friend, R. H.; Kim, J.-S. *J. Am. Chem. Soc.* **2005**, *127*, 12890−12899.
(27) Gurau, M. C.; Delongchamp, D. M.; Vogel, B. M.; Lin, E. K.; Fischer, D. A.; Sambasivan, S.; Richter, L. J. *Langmuir* **2007**, *23*, 834−842.
(28) Zhang, X.; Richter, L. J.; DeLongchamp, D. M.; Kline, R. J.; Hammond, M. R.; McCulloch, I.; Heeney, M.; Ashraf, R. S.; Smith, J. N.; Anthopoulos, T. D.; Schroeder, B.; Geerts, Y. H.; Fischer, D. A.; Toney, M. F. *J. Am. Chem. Soc.* **2011**, *133*, 15073−15084.
(29) DeLongchamp, D. M.; Kline, R. J.; Fischer, D. A.; Richter, L. J.; Toney, M. F. *Adv. Mater.* **2011**, *23*, 319−337.
(30) Garreau, S.; Leclerc, M.; Errien, N.; Louarn, G. *Macromolecules* **2003**, *36*, 692−697.
(31) Wetzelaer, G.-J. A. H.; Kuik, M.; Olivier, Y.; Lemaur, V.; Cornil, J.; Fabiano, S.; Loi, M. A.; Blom, P. W. M. *Phys. Rev. B: Condens. Matter Mater. Phys.* **2012**, *86*, 165203.
(32) Schuettfort, T.; Huettner, S.; Lilliu, S.; Macdonald, J. E.; Thomsen, L.; McNeill, C. R. *Macromolecules* **2011**, *44*, 1530−1539.
(33) Giussani, E.; Fazzi, D.; Brambilla, L.; Caironi, M.; Castiglioni, C. *Macromolecules* **2013**, *46*, 2658−2670.
(34) Gann, E.; McNeill, C. R.; Szumilo, M.; Sirringhaus, H.; Sommer, M.; Maniam, S.; Langford, S. J.; Thomsen, L. *J. Chem. Phys.* **2014**, *140*, 164710.
(35) Schuettfort, T.; Thomsen, L.; McNeill, C. R. *J. Am. Chem. Soc.* **2013**, *135*, 1092−1101.
(36) Kipnusu, W. K.; Kossack, W.; Iacob, C.; Jasiurkowska, M.; Sangoro, J. R.; Kremer, F. *Z. Phys. Chem.* **2012**, *226*, 797−805.
(37) Jasiurkowska, M.; Kossack, W.; Ene, R.; Iacob, C.; Kipnusu, W. K.; Papadopoulos, P.; Sangoro, J. R.; Massalska-Arodz, M.; Kremer, F. *Soft Matter* **2012**, *8*, 5194−5200.
(38) Kossack, W.; Papadopoulos, P.; Parkinson, M.; Prades, F.; Kremer, F. *Polymer* **2011**, *52*, 6061−6065.
(39) Kossack, W.; Papadopoulos, P.; Heinze, P.; Finkelmann, H.; Kremer, F. *Macromolecules* **2010**, *43*, 7532−7539.
(40) Warner, M.; Terentjev, E. M. In *Liquid Crystal Elastomers*; Birman, J., Edwards, S. F., Friend, R., Rees, M., Sherrington, D., Veneziano, G., Eds; Clarendon Press: Oxford, 2009.
(41) Ikeda, R.; Chase, B.; Everall, N. J. In *Vibrational Spectroscopy of Polymers: Principles and Practice*; Everall, N. J., Chalmers, J. M., Griffiths, P. R., Eds; John Wiley & Sons Ltd: Chichester, 2007.

DOI: 10.1021/jacs.5b01755
J. Am. Chem. Soc. 2015, 137, 6034−6043